The Role of High- and Low-Frequency Dynamics in Blocking Formation

HISASHI NAKAMURA

Department of Earth and Planetary Physics, University of Tokyo, Tokyo, Japan

MOTOTAKA NAKAMURA*

Center for Meteorology and Physical Oceanography, Massachusetts Institute of Technology, Cambridge, Massachusetts

JEFFREY L. ANDERSON

Geophysical Fluid Dynamics Laboratory/NOAA, Princeton University, Princeton, New Jersey

(Manuscript received 9 April 1996, in final form 11 September 1996)

ABSTRACT

Time evolutions of prominent blocking flow configurations over the North Pacific and Europe are compared based upon composites for the 30 strongest events observed during 27 recent winter seasons. Fluctuations associated with synoptic-scale migratory eddies have been filtered out before the compositing. A quasi-stationary wave train across the Atlantic is evident during the blocking amplification over Europe, while no counterpart is found to the west of the amplifying blocking over the North Pacific. Correlation between the tropopause-level potential vorticity (PV) and meridional wind velocity associated with the amplifying blocking is found to be negative over Europe in association with the anticyclonic evolution of the low-PV center, but it is almost zero over the North Pacific. Feedback from the synoptic-scale eddies, as evaluated in the form of 250-mb geopotential height tendency due to the eddy vorticity flux convergence, accounts for more than 75% of the observed amplification for the Pacific blocking and less than 45% for the European blocking. This difference is highlighted in two types of ''contour advection with surgery'' experiments. In one of them PV contours observed four days before the peak blocking time were advected by composite time series of the low-pass-filtered observational wind, and in the other experiment they were advected by the low-pass-filtered wind from which the transient eddy feedback evaluated as above had been removed at every time step. Hence, the latter data should be dominated by low-frequency dynamics. For the European blocking both experiments can reproduce the anticyclonic evolution of low-PV air within a blocking ridge as observed. For the Pacific blocking, in contrast, the observed intrusion of low-PV air into the higher latitudes cannot be reproduced without the transient feedback. Furthermore, in a barotropic model initialized with the composite 250-mb flow observed three days before the peak time, a simulated blocking development over the North Pacific is more sensitive to the insertion of the observed transient feedback than that over Europe. These results suggest that the incoming wave activity flux associated with a quasi-stationary Rossby wave train is of primary importance in the blocking formation over Europe, whereas the forcing by the synoptic-scale transients is indispensable to that over the North Pacific.

1. Introduction

Owing to its longevity and large amplitude, a blocking flow configuration can cause prolonged anomalous weather situations over certain extratropical regions. Therefore, it has been a primary interest of many synoptic and dynamical meteorologists for decades. In their pioneering studies, Berggren et al. (1949) and Rex (1950) suggested that interaction with migratory, synoptic-scale transient eddies may be instrumental in the blocking formation. The interaction has been recognized to be an important mechanism for the maintenance of blocking anticyclones (Green 1977; Illari and Marshall 1983; Dole 1986; Mullen 1987; Holopainen and Fortelius 1987). Recent numerical simulations demonstrated the possibility that the interaction may lead to the formation of blocking anticyclones (Shutts 1983; Metz 1986; Haines and Marshall 1987; Vautard and Legras 1988). In fact, the amplification of some blocking anticyclones follows abnormally high activity of high-frequency, migratory eddies upstream (Nakamura and Wallace 1990, 1993; Neilley 1990), characterized synoptically by explosive cyclogenesis (Colucci 1985, 1987; Crum and Stevens 1988; Konrad and Colucci 1988).

* Current affiliation: Department of Earth, Atmospheric and Planetary Sciences, Massachusetts Institute of Technology, Cambridge, Massachusetts.

Corresponding author address: Dr. Hisashi Nakamura, Department of Earth and Planetary Physics, Faculty of Science, University of Tokyo, 2-11-16 Yayoi, Bunkyo-ku, Tokyo 113, Japan.
E-mail: hisashi@geoph.s.u-tokyo.ac.jp

Interacting with an amplifying blocking ridge as they migrate, the high-frequency transient eddies exert a positive feedback that acts to reinforce the ridge mainly through vorticity fluxes (Tsou and Smith 1990; Nakamura 1990). The importance of the transient eddies in the blocking development was suggested also by numerical forecasting experiments (Chen and Juang 1992; Kimoto et al. 1992) and by analyses of blocking events simulated in general circulation models (GCMs; Blackmon et al. 1986; Higgins and Schubert 1994).

However, it has not been established yet that the majority of the observed blocking events form due solely to the forcing by the high-frequency transient eddies. Some of the most recent studies suggest that dynamical processes with timescales longer than those of synoptic-scale eddies may also be operative in the blocking formation. In a long integration of a two-layer GCM by Stewart (1993), the formation of persistent anticyclonic anomalies tends to follow the occurrence of quasi-stationary wave trains upstream. H. Nakamura (1994) showed that the amplification of the strongest blocking events observed over Europe is indeed associated with a quasi-stationary Rossby wave train across the North Atlantic. He also showed that another wave train emanating downstream becomes evident as the blocking ridge weakens. He hypothesized that the local absorption of the wave activity and its reemission, in association with temporary ''obstruction of Rossby wave propagation,'' lead to the formation and the following decay of the strong blocking ridge over Europe, respectively. Indeed, the observed potential vorticity (PV) evolution, including the anticyclonic evolution associated with the blocking over Europe, was reproduced reasonably well in ''contour advection with surgery'' (CAS) experiments, which M. Nakamura (1994) applied to several blocking patterns using the low-pass-filtered observational and GCM-generated wind. He hypothesized that the observed and GCM-simulated blocking events he examined are associated with the breaking of quasi-stationary Rossby waves. These results are consistent with recent diagnostic studies that suggest that the vorticity (or PV) advection by the low-pass-filtered flow may be as important as the transient feedback in the blocking formation (Nakamura 1990; M. Nakamura 1994).

Still, it is not clear that low-frequency dynamics such as the temporary obstruction of Rossby wave propagation is strong enough to form blocking anticyclones by itself in the real atmosphere. Difficulties in diagnosing low-pass-filtered fields arise from the contribution of the continual forcing by high-frequency transient eddies to the steady amplification of the blocking, which is hardly distinguishable from the contribution of the low-frequency dynamics. Suppose a blocking anticyclone begins to develop in a westerly jet along which high-frequency eddies are migrating. The contribution of the low-frequency (internal) dynamics is included entirely in the advection of low-pass-filtered PV by the low-pass-filtered wind. The low-frequency dynamics should be the sole contributor to the advection unless the eddies interact with the blocking and exert a feedback upon it. In the presence of such feedback, however, the wind and vorticity fields associated with the blocking, even if low-pass filtered, should evolve more or less differently from how they would without such feedback. In other words, the advection of low-pass-filtered vorticity or PV by the low-pass-filtered flow includes the effect of the feedback by the high-frequency transients in addition to the effect of the low-frequency dynamics. In the diagnostic studies mentioned above, therefore, the contributions from these two kinds of dynamics to the blocking development were not completely separated.

In the present study, we will attempt to isolate the role of low-frequency dynamics from that of high-frequency transients in the formation of strong blocking anticyclones. First we will compare the composited life cycles of the blocking at two different locations: one over Europe and the other over the North Pacific. It will be shown that the convergence of the wave activity density flux associated with low-frequency dynamics is substantially stronger during the European blocking onset, whereas the high-frequency transients exert a much stronger feedback upon the evolution of the Pacific blocking. These differences will be confirmed using CAS and barotropic model experiments. In each of the experiments we use two time series of wind to advect vorticity or PV distributions observed during the blocking onset: one is the low-pass-filtered composites of the observed upper-level wind, and the other is the low-pass-filtered composites with the forcing by the high-frequency transients through vorticity flux convergence removed. The latter sequence should be dominated by the low-frequency dynamics because at the tropopause level the barotropic forcing imposed there by the transients (which is counteracted by the remote forcing due to the heat fluxes at the lower levels) sets an upper limit on the net transient forcing (Lau and Nath 1991; Branstator 1992). Hence, our approach should lead to a conservative measure of the contribution from the low-frequency dynamics to the blocking development.

2. Data and analysis method

The data used in this study are gridded fields of 250-mb geopotential height (Z_{250}) and 300- and 200-mb potential temperature (θ_{300} and θ_{200}) for 0000 and 1200 UTC each day based on the operational analyses by the National Meteorological Center (NMC, now the National Centers for Environmental Prediction) for the period 1965–1992. These twice-daily data are available in the archive at the National Center for Atmospheric Research. Twice-daily fields of potential vorticity (PV) at the tropopause level (PV_{250}) have been constructed from the unfiltered gridded fields by applying an approximate form of the Ertel PV to the 250-mb isobaric surface (Nakamura and Wallace 1993). With this approximation we could afford to compute the sequence of PV_{250} with 12-h intervals for the 27-yr period. Unlike the Ertel PV, however, PV_{250} is a conservative quantity in the three-

dimensional sense but not on the pressure surface. Still, it should give us an approximation of the horizontal distribution of the Ertel PV at the tropopause level because the 250-mb surface in the extratropics is close to an isentropic surface of approximately 330 K in the climatological mean and even in the vicinity of a strong blocking ridge (Hoskins et al. 1985).

In order to prevent erroneous data from being mistakenly selected as strong anomaly events, the following precautionary checking of the data quality was performed. First we recorded when and where the data values deviated from the corresponding climatological means by more than a threshold or whether they exhibited 12-h changes larger than another threshold. The thresholds for these two types of ''suspicious'' data were prescribed as six times the local standard deviation of the data values themselves and seven times the local standard deviation of the 12-h tendency, respectively, obtained for each calendar month. Next, after visual inspection, any of the suspicious data that evolved discontinuously in time were identified as low-quality data. These were found mostly in the height fields to the south of 30°N. The same checking was applied to each of the suspicious data periods that have been identified through an independent examination by Trenberth and Olson (1988). A plausible field was recovered by applying a linear spatial interpolation to a confined region of the contaminated data. However, a single field as a whole was eliminated from our dataset when the contamination was widespread (say, 3000 km in diameter). Finally, each of the missing data periods, including the eliminated fields, was interpolated linearly in time before the filtering described below. Any of these periods that span three consecutive days or longer were not used in our analysis. They account only for about 1.5% of the whole dataset.

In the present study, we focus on the slow evolution of blocking flow configurations, which has been isolated by digital filtering from fluctuations associated with the synoptic-scale migratory eddies whose timescales are shorter than 1 week. These migratory eddies are referred to as high-frequency transient eddies or transients in this study, and regions within which these eddies are particularly strong are referred to as storm tracks. A recursive, six-pole, tangent-Butterworth filter with the half-power cutoff of 8 days was applied to the data sequence as a low-pass filter (Kaylor 1977). The 8-day low-pass-filtered fields do not exclude stationary blocking ridges that are built up from the undisturbed situation within 3 days and then undergo a rapid decay for the next 3 days. Dole (1983) showed that such short-lived episodes of strong stationary anomalies occur more frequently than more persistent ones.

Unlike in Nakamura and Wallace (1993), we will not analyze the migratory high-frequency eddy components themselves. Rather, it is of interest to examine how their amplitudes are modulated and how their feedback on the flow with longer timescales is altered as blocking ridges amplify and then decay. The slowly modulated amplitude of the transient eddies at a particular location was defined as the low-pass-filtered intensity of the fluctuations in the wind component perpendicular to the low-pass-filtered local wind vector at the 250-mb level [VH_{250}; see appendix A for details]. This definition was based upon the fact that wind fluctuations perpendicular to the instantaneous local jet axis, determined as above from the slowly varying wind component, are associated mostly with those eddies. The VH_{250} is a local measure of the instantaneous amplitude (or activity) of the eddies, and regions with large values correspond to so-called storm tracks. The high-frequency transients exert a feedback in terms of horizontal heat and vorticity fluxes upon the slowly varying flows on which they are embedded. The slowly varying flows include the climatological mean flow and the low-pass-filtered anomalies associated with the blocking. In this study only the barotropic feedback through the vorticity fluxes is analyzed. It has been evaluated as the low-pass-filtered tendency of the 250-mb geopotential height induced solely by the anomalous vorticity flux convergence associated with the transient eddies at that level [$(\partial Z^*_{250}/\partial t)_{\mathrm{HFT}}$; see appendix B for details]. At the tropopause level, the barotropic feedback generally acts to strengthen the basic flow, which is counteracted by the baroclinic feedback through the heat fluxes at lower levels (Lau and Holopainen 1984; Lau and Nath 1991). Therefore, $(\partial Z^*_{250}/\partial t)_{\mathrm{HFT}}$ may be regarded as an upper bound on the total eddy feedback since the former tends to overestimate the latter.

Strong blocking episodes for locations of interest were identified as follows. First, every winter season (November–April), the maximum value of the 8-day low-pass-filtered Z_{250} anomalies observed within 500 km of that location was recorded every day. (Justification of the particular choice of 500 km will be given later.) A local anomaly of a given variable for a particular time was defined as its departure from the local value of the climatological-mean annual cycle for the corresponding calendar day. The annual cycle was obtained as the average of its 31-day running-mean fields over the 27-yr period (1965 summer through 1992 spring). Only the top 4% of the strongest positive (i.e., anticyclonic) anomalies at a given location were recognized to be associated with blocking events. The peak time of the blocking was recorded for any of these events if observed within the 150-day winter season (15 November–13 April), and the strength of a blocking event was defined as the Z_{250} anomaly at the peak time.

We composited the 15 strongest blocking events[1]

[1] The 30 strongest anticyclonic events at 54°N, 10°E are all called blocking or blocks in this study since they all satisfy Anderson's (1993) criterion, as suggested by the fact that the composite for the 31st to 45th strongest cases also satisfies the criterion. Almost all the 30 strongest anticyclonic events at 56°N, 160°W are called blocking because the composite for the 26th to 30th strongest cases satisfies the criterion. Furthermore, each of the composite patterns for E1, P1, E2, and P2 is called blocking according to the criterion.

sampled for each of two reference grid points: 54°N, 10°E and 56°N, 160°W (hereafter cited as E1 and P1, respectively). We also composited the 16th–30th strongest cases for each of the reference points (hereafter cited as E2 and P2, respectively). The blocking development at the latter grid point, located at the exit of the Pacific storm track, suggests strong interactions with the high-frequency eddies without any significant indication of incoming Rossby waves (Nakamura and Wallace 1990). In contrast, incoming Rossby waves are apparent during the blocking development at the former grid point (H. Nakamura 1994; M. Nakamura 1994). We intend to differentiate these two types of blocking formation by evaluating the contributions from the high-frequency eddies. Here E1 and E2 are chosen as typical examples of blocking formation in which the low-frequency dynamics is dominant but not as examples of the traditional Atlantic block.

As shown below, several anomaly centers associated with a blocking event tend to be distributed far upstream or downstream of the primary anticyclonic anomalies, particularly during the onset and decay stages. Compositing, which emphasizes systematic signals among the 15 events, was necessary to isolate those associated anomaly centers that are not as strong as the primary one. Otherwise, they may be hidden by other anomalies that are not associated with the blocking. In order to sharpen the composited signatures, the entire field was, if necessary, translated before compositing in such a manner that the strongest anticyclonic anomaly center in Z_{250} at the peak time of each blocking event coincided with the reference point (Nakamura 1990). This translation was performed by rotating the entire field along the great circle that connects the anomaly center and the reference point. The composited signatures keep their geographical identities since this translation shifts the fields by less than 500 km, a distance much smaller than the spatial scales of blocking ridges. The same translation was applied for each event to all variables for all time lags relative to the peak blocking time.

3. Observed evolution of blocking

Figure 1 shows the composited time evolution of the 250-mb circulation for E1.[2] The total low-pass-filtered Z_{250} field is characterized by a closed anticyclonic circulation in association with a strong blocking ridge over Europe. The westerly jet over the Atlantic and the weak westerlies over the Eurasian continent constitute strong diffluence over western Europe, which weakens later as a downstream trough deepens. The total field of PV_{250} exhibits distinctive anticyclonic evolution that commences with the intrusion of low-PV air into the diffluent region from the southwest. The resulting low-PV center moves slowly northeastward where the meridional wind (v) is positive (i.e., from the south), until it reaches the northern fringe of the weak-westerly region by the peak time. Then, as the blocking decays, the center gradually moves southeastward where v is negative. Meanwhile, a tongue of high-PV air that appears to intrude to the south of the blocking anticyclone becomes meridionally compressed and then develops into the smaller structures. All of these characteristics in the PV evolution are associated with statistically significant PV anomalies. Though less apparent, the primary anticyclonic anomaly in Z_{250} rotates anticyclonically, as observed during a blocking episode over the northeastern Atlantic (Mak 1991).

Anticyclonic movement of the low-PV center was also observed in isentropic PV maps during a blocking episode over the North Sea (Shutts 1986). Such movement signifies the correlation between PV and v changing its sign during a blocking episode. The correlation is equivalent to the divergence of the extended Eliassen–Palm (E–P) flux (Hoskins et al. 1983; Trenberth 1986). Since the flux corresponds to the wave activity density flux associated with Rossby wave propagation, the PV–v correlation changing from negative to positive may be interpreted as the convergence of the wave activity flux into the amplifying blocking ridge followed by the divergence from the decaying ridge. In fact, the Z_{250} anomalies are characterized by quasi-stationary wavy signatures, one over the Atlantic in the amplification stage and another over Eurasia in the decay stage. The hypothesis that they are disturbances in association with Rossby waves can be substantiated by applying Plumb's (1986) formulation of the wave activity density flux to the composited anomaly fields of Z_{250}, PV_{250}, θ_{300}, and θ_{200}.[3] In this estimation, their wintertime climatological-mean fields were used as the zonally varying basic state on which the waves are embedded, and the geostrophic wind obtained from Z_{250} with the latitude-dependent Coriolis parameter was used in place of the observed

[2] Part of the figure has already been presented in H. Nakamura (1994) and is duplicated here so that the reader can easily find its relationship with the evolution of newly added variables such as VH_{250}. Also added to the figures in this study is an indication of statistical significance of the composited anomalies as measured by the t statistic.

[3] The three-dimensional flux of wave activity density defined by Plumb (1986) becomes independent of the spatial phase of wavy disturbances after ensemble average is taken, for example, by averaging many realizations of such disturbances with various phase alignments that happened over a long time period. This averaging is equivalent to incorporating the contribution of the same wavy patterns but with the phase shifted by one-quarter wavelength. Hence, strictly speaking, Plumb's formulation cannot be applied to composited stationary anomaly patterns as in Fig. 1. Nevertheless, simple spatial smoothing, which has an effect equivalent to the phase averaging, has been applied to the flux fields based on the anomaly patterns in Fig. 1, so that they give us some idea of which direction the wave activity is propagating and how strong it is. It should be stressed that the flux patterns depicted in Fig. 1 only give a qualitative measure of the Rossby wave propagation.

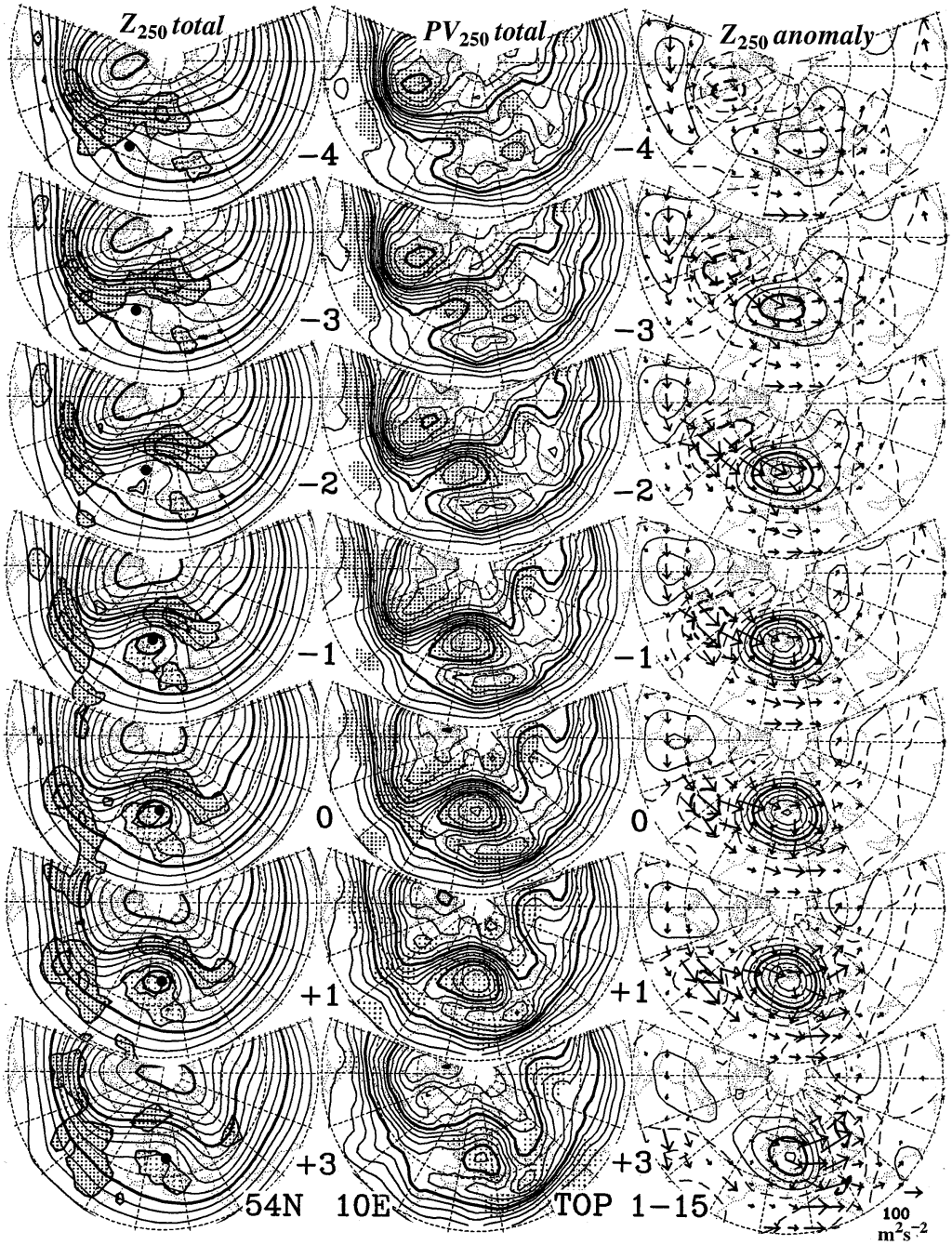

FIG. 1. Composite time evolution of Z_{250}, PV_{250}, and anomalous Z_{250} fields associated with the 15 strongest blocking events at 54°N, 10°E in 27 winter seasons. Composites of low-pass-filtered fields are presented for days relative to the peak time as indicated (negative and positive values signify the amplification and decay stages, respectively). In Z_{250} (left) and PV_{250}, (middle) composites, VH_{250} anomalies with at least 3 m s^{-1} in magnitude and PV_{250} anomalies with at least 95% significance are indicated by shading, respectively. Closed circles in the left column indicate the low-PV centers. Wave activity density flux based on the composite anomalies is superimposed (arrows; scaling on the lower-right corner) upon Z_{250} anomalies (right). Contour lines: every 100 m (heavy lines for 9500, 10 000, and 10 500) for Z_{250}; ±3 and ±6 m s^{-1} for VH_{250} anomalies (heavy and light shading signifies above and below normal high-frequency transient activity, respectively); every 0.4 PVU (=10^{-6} m^2 s^{-1} K kg^{-1}; heavy lines for 2, 4, and 6) for PV_{250}; ±30, ±90, ±150, ±210 m, . . . (heavy lines for ±150 and ±450) for Z_{250} anomalies (dashed and solid lines signify cyclonic and anticyclonic anomalies, respectively). In each panel the area 20°–90°N, 100°W–120°E is plotted with 10°E in front.

wind. Figure 1 (right column) indeed indicates that the wave activity density flux across the North Atlantic converges into the weak-westerly region within the amplifying blocking ridge, and no signature of wave propagation is evident farther downstream until the blocking reaches its peak. After the peak, the wave activity density flux becomes apparent downstream of the blocking associated with another wave train. This rather abrupt release of the wave activity downstream is suggestive of temporary obstruction of the wave propagation across the blocking region, which is probably caused by the weakening of the westerlies due to the amplification of the anticyclonic anomalies (H. Nakamura 1994). Once the weakening of the westerlies begins, the wave activity starts accumulating where the flux converges, which results in the amplification of the blocking and the further weakening of the westerlies.

The composite E2 exhibits essentially the same time evolution as E1 (not shown). The only noticeable difference is a weaker signature of the temporary obstruction of the wave propagation in E2, as noted by H. Nakamura (1994). The wave activity density flux extends downstream across the primary anticyclonic anomaly, which is less elongated zonally than that for E1, even around the peak time of the blocking.

Contrasting time evolution is observed in the composite maps for P1 (Fig. 2). Unlike for E1 and E2, no significant signature of quasi-stationary wavy disturbances is found during the amplification stage. In fact, the PV–v correlation in the vicinity of the amplifying blocking ridge is almost zero, which is consistent with no incoming flux of the wave activity density from upstream. Black (1997) also found little evidence of the incoming flux of wave activity density during persistent anticyclonic anomaly events over the North Pacific. Then, downstream emanation of the flux concomitant with the formation of a quasi-stationary wave train becomes apparent over North America even before the peak time. Again, this emanation is consistent with the positive PV–v correlation, which is yielded by the gradual eastward shift of the low-PV center and the slowly retrograding pressure ridge as the blocking reaches its peak and then decays. Composites for P2 exhibit essentially the same time evolution as P1 (not shown). The only noticeable difference is that incipient anticyclonic anomalies, observed over the North Pacific 4 or 6 days before the peak time, are about 40% weaker for P2 than for P1. These two sets of composites reveal no indication of significant contribution from incoming Rossby waves to the blocking formation.

4. Contribution of high-frequency transient eddies

Previous studies listed in section 1 indicate that the high-frequency transient eddies exert a positive feedback on amplifying blocking ridges over the North Pacific and Atlantic. In this section the importance of the transient eddy feedback upon the blocking formation is examined. Patterns of the anomalous eddy activity, as measured by VH_{250} in association with the time evolution of E1 and P1, are shown in the left columns of Figs. 1 and 2, respectively. Upstream enhancement of the activity is evident during the early amplification stage of the blocking for both E1 and P1. The enhancement is somewhat less apparent in E2 and P2. As the westerlies become split due to the amplification of the blocking, the eddy activity tends to be suppressed in the vicinity of the ridge and enhanced to the north of it. The above-normal activity is also evident to the south of the ridge over the Pacific along the southern branch of the westerlies. The amplitude modulation of high-frequency transient eddies depicted in the evolution of VH_{250} during the blocking formation is consistent with that in the previous studies (Nakamura and Wallace 1990; Neilley 1990).

The patterns of anomalous VH_{250} shown in Figs. 1 and 2 imply that anomalous divergence of the extended E–P flux (not shown) associated with the anomalously active storm track extending to the north, and even to the south for P1, of an amplifying blocking ridge acts to reinforce the local westerlies. They also imply that the anomalous convergence of the flux associated with the anomalously weak storm track in the vicinity of the ridge acts in the opposite sense (Hoskins et al. 1983; Trenberth 1986). Hence, the transient eddies, whose activity is modulated as the blocking ridge strengthens, act to reinforce the ridge and the westerly split. In order to evaluate this positive feedback quantitatively, time evolution composites of $(\partial Z^*_{250}/\partial t)_{\mathrm{HFT}}$ for E1 and P1 are presented in the middle columns of Figs. 3 and 4, respectively. In both cases, the transient eddies indeed act to strengthen the existing quasi-stationary anticyclonic anomalies throughout the life cycle of the blocking. The same kind of transient forcing is also observed for E2 and P2 (not shown). The overall tendency of the transient forcing is consistent with the findings in the previous studies mentioned above. The anticyclonic forcing by the transient eddies exhibits high statistical significance in each of the composites, which implies that the forcing pattern is fairly coherent from one event to another for both blocking locations.

However, the forcing over the North Pacific is much stronger and more in-phase with the anticyclonic anomalies associated with the blocking than over Europe. Hence, more efficient positive feedback is deposited into the blocking over the North Pacific. This difference is quantified by estimating the total positive feedback the high-frequency transients exert upon the primary anticyclonic anomalies during the amplification stage of the blocking. Specifically, at each time lag the composited $(\partial Z^*_{250}/\partial t)_{\mathrm{HFT}}$ was averaged over the domain around the primary anticyclonic center within which the composited Z_{250} anomalies are greater than one-half of their maximum value (at the anomaly center), so that the forcing was sampled following the slowly moving anomaly center. The averaged feedback was then ac-

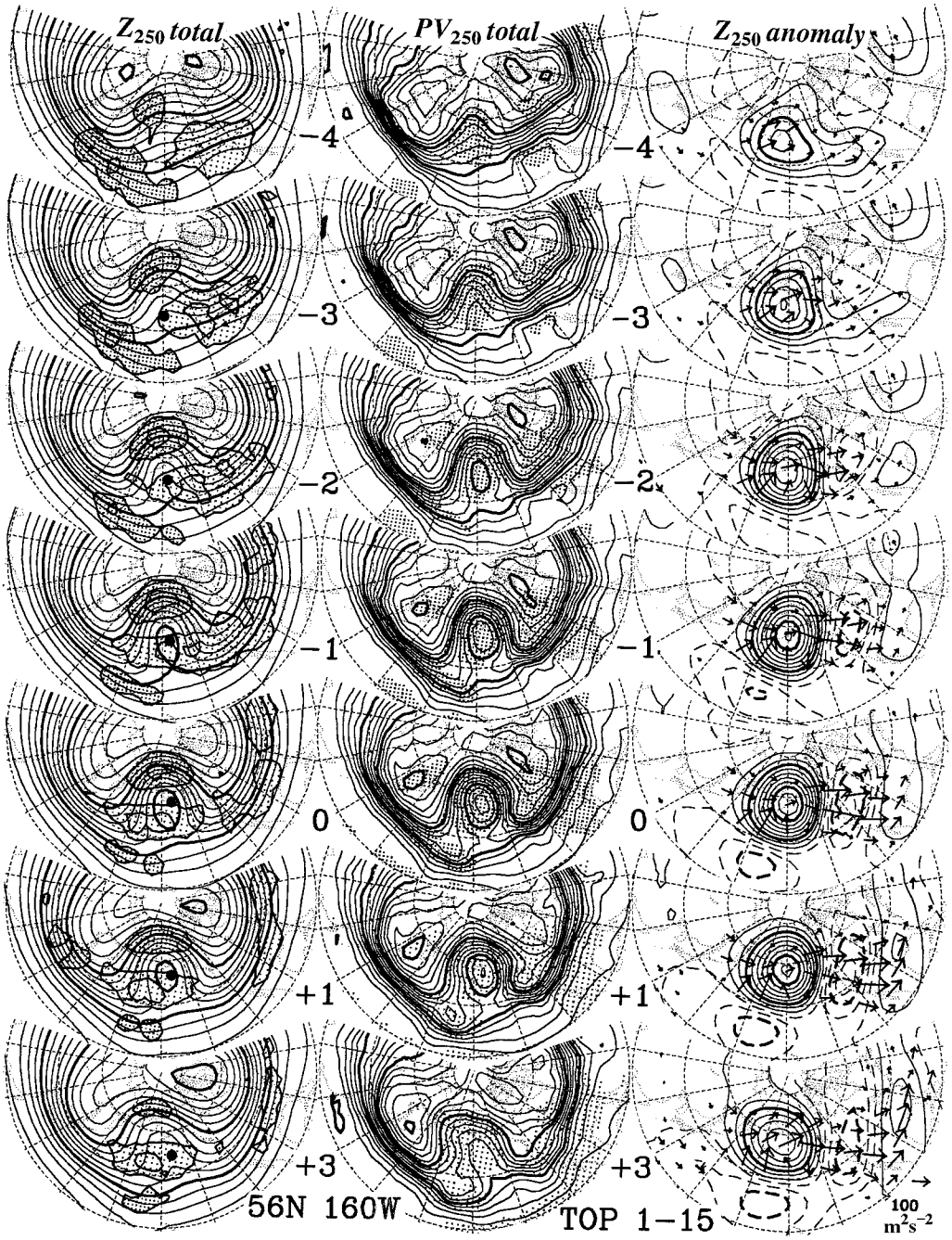

FIG. 2. As in Fig. 1 but for 56°N, 160°W. In each panel the area 20°–90°N, 90°E–50°W is plotted with 160°W in front.

cumulated over the 4-day period from day −4 to day −0.5, with 12-h intervals in lag. Meanwhile, at each of day −4 and day 0 (peak), Z_{250} anomalies themselves were averaged over the same domain as defined above for averaging the transient forcing for the corresponding lag. The difference in the spatially averaged Z_{250} between these two lags ($\Delta Z^*_{\mathrm{OBS}}$) is regarded as a measure of the observed amplification of the blocking. This measure and the transient forcing accumulated over the 4-day amplification period ($\Delta Z^*_{\mathrm{HFT}}$) are both listed in Table 1. It is apparent that $\Delta Z^*_{\mathrm{HFT}}$ over Europe is less than one-half of that over the North Pacific, though $\Delta Z^*_{\mathrm{OBS}}$ for the European blocking is 10%–15% smaller than that for the Pacific blocking. The transient forcing accounts only for 33%–45% of $\Delta Z^*_{\mathrm{OBS}}$ over Europe, whereas it accounts for 77%–97% of $\Delta Z^*_{\mathrm{OBS}}$ over the Pacific. Recalling that $\Delta Z^*_{\mathrm{HFT}}$ can be regarded as an upper bound on the net contribution from the transients, we can conclude that the transient forcing alone, in general, cannot form strong blocking ridges over Europe, per-

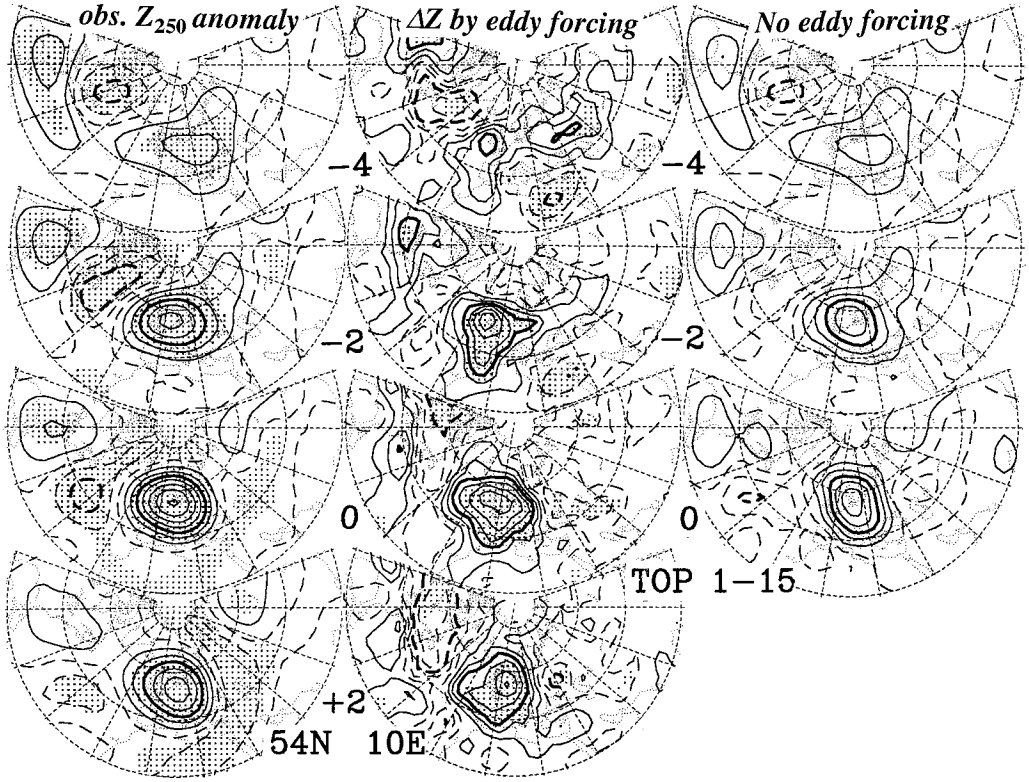

FIG. 3. Composite time evolution of Z_{250} anomalies (left) and barotropic forcing by high-frequency transients $(\partial Z^*_{250}/\partial t)_{\mathrm{HFT}}$ (middle), associated with the 15 strongest blocking events at 54°N, 10°E in 27 winter seasons for days relative to the peak time as indicated (negative and positive values signify the amplification and decay stages, respectively). Presented in the right column is hypothetical evolution of Z_{250} anomalies due only to the low-frequency dynamics, as estimated by subtracting $(\partial Z^*_{250}/\partial t)_{\mathrm{HFT}}\Delta t$ from the composited evolution every 12 h (i.e., $\Delta t = 0.5$ day). In the left and middle columns, anomalies with at least 95% significance are indicated by shading. Contour lines: ±30, ±90, ±150, ±210 m, . . . (left and right; heavy lines for ±150 and ±450); ±5, ±15, ±25, ±35 m day^{-1}, . . . (middle; heavy lines for ±25 and ±75); dashed and solid lines signify cyclonic and anticyclonic anomalies, respectively. In each panel the area 20°–90°N, 100°W–120°E is plotted with 10°E in front.

haps because the Atlantic storm track is too far upstream. The converging flux of wave activity density associated with the quasi-stationary wave train across the Atlantic must be a primary contributor to the formation of strong blocking there. In contrast, the transient forcing appears to be strong enough to form strong blocking ridges over the North Pacific, which is very close to the exit of the Pacific storm track.

The substantial difference in the blocking formation over Europe and the Pacific was further verified in the time evolution of the low-frequency anomalies from which the feedback from the high-frequency transients had been removed. First, a field of time tendency observed in Z_{250}, that is, $(\partial Z^*_{250}/\partial t)_{\mathrm{OBS}}$, was obtained for each of the half-day lag intervals ($\Delta t = 0.5$ day) by taking the difference in the Z_{250} anomaly composites between the two adjacent lags. Then, the Z_{250} anomaly composite at day −4 was taken as the initial field, upon which the difference field $[(\partial Z^*_{250}/\partial t)_{\mathrm{OBS}} - (\partial Z^*_{250}/\partial t)_{\mathrm{HFT}}]\Delta t$ for each of the individual lag intervals was successively accumulated to yield a hypothetical field of blocking amplification due solely to the low-frequency dynamics. For example, a hypothetical field for day −3 was obtained by accumulating the difference fields for the lag intervals between days −4 and −3.5 and between days −3.5 and −3 on the initial field (at day −4). The underlying assumption here is that $(\partial Z^*_{250}/\partial t)_{\mathrm{HFT}}$ is the strongest forcing the transient eddies could exert on the low-frequency anomalies. The hypothetical time evolutions of Z_{250} anomaly that obtained ($\tilde{Z}^*_{250}$) based on E1 and P1 are shown in the right columns of Figs. 3 and 4, respectively, which should be compared with the observational counterpart in the left columns. Though somewhat weaker and compressed zonally, the amplification of the primary anticyclonic anomalies associated with the European blocking is well reproduced in the time evolution of $\tilde{Z}^*_{250}$. The peak amplitude of the primary anomaly center is only about 60 m smaller than observed, and the center is located near the observed position. In contrast, the peak amplitude of the primary anomaly center of the Pacific blocking is underestimated in $\tilde{Z}^*_{250}$ by as much as about 200 m, and its position is

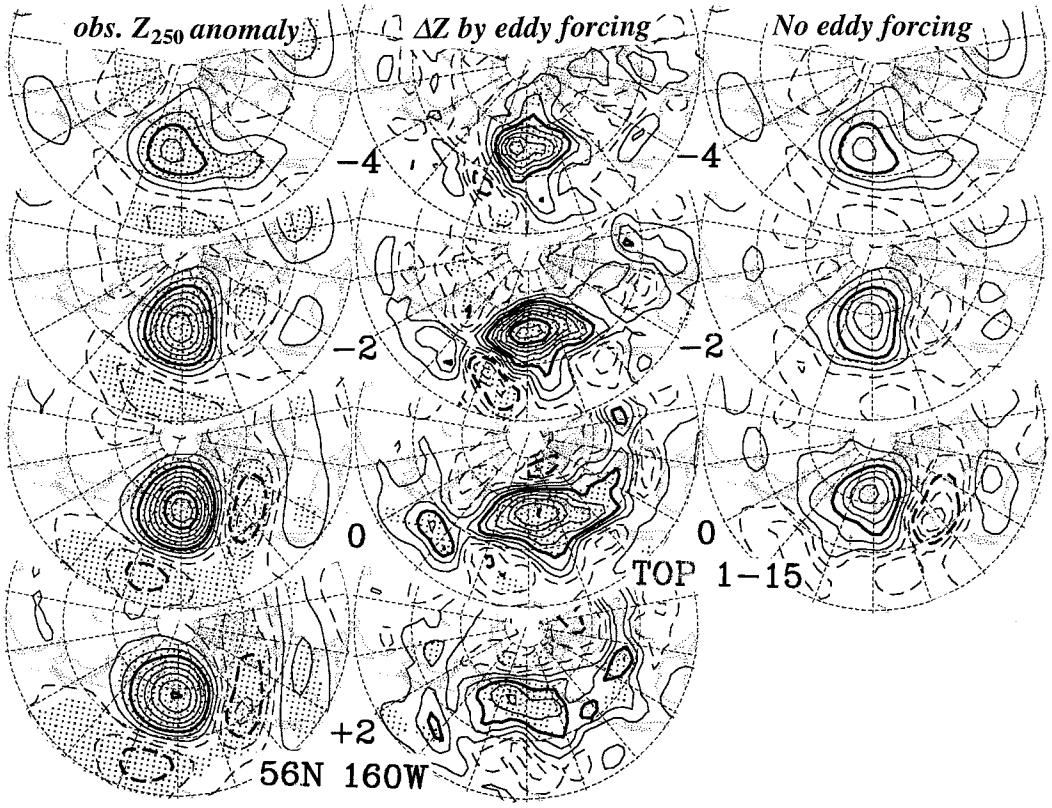

FIG. 4. As in Fig. 3 but for 56°N, 160°W. In each panel the area 20°–90°N, 90°E–50°W is plotted with 160°W in front.

shifted considerably to the northwest of the observed center. These results suggest that a strong blocking anticyclone would emerge over Europe even without the transient forcing but would not over the North Pacific. It should be noted that a wave train downstream of the Pacific blocking ridge is reproduced without the transient forcing, which indicates that it is a manifestation of the emanation of quasi-stationary Rossby waves.

5. CAS experiments

The substantial difference in the importance of the high-frequency transient forcing in the blocking formation discussed in the preceding section can be visualized clearly by the following experiments with ''contour advection with surgery'' (CAS) developed by Waugh and Plumb (1994). CAS uses wind data to advect contours of constant PV values to predict their future locations. The wind data are linearly interpolated in time and space to obtain the advecting wind on the contours. When the contours develop features smaller than a certain prescribed scale or features with curvature greater than a certain prescribed threshold, CAS smooths out the contours by removing those features and reconnecting them in an appropriate manner (see Waugh and

TABLE 1. Contribution of high-frequency transients (HFTs) to observed time evolution of geopotential height anomalies (ΔZ^*_{OBS}) during the blocking formation over Europe (upper) and the North Pacific (lower). For each of the regions, statistics based on the composites for the 15 strongest events and the next 15 strongest events are listed separately. Observed growth ΔZ^*_{OBS} (fourth column) was evaluated by subtracting the anticyclonic anomaly strength at day −4 (second column) from that at the peak blocking time (day 0; third column). The strength of the anticyclonic anomalies was evaluated by averaging Z_{250} anomalies in the vicinity of the primary anomaly center. The contribution of the transient eddies (sixth column) is the ratio of their barotropic forcing of the geopotential height field (fifth column) to ΔZ^*_{OBS}. The forcing, defined as $(\partial Z^*_{250}/\partial t)_{HFT}$ in the text, was averaged spatially in the above-mentioned manner at each of the half-day lags and then accumulated, after being multiplied by that time interval, from day −4 to day −0.5 (see text for more details).

	Amplitude rank	Z^* (m) day −4	Z^* (m) peak	ΔZ^* (m) obs.	HFT forcing (m)	HFT contribution
54°N, 10°E	1–15	81	287	206	93	45%
(Europe)	16–30	84	259	175	60	34%
56°N, 160°W	1–15	169	411	242	187	77%
(North Pacific)	16–30	146	338	192	187	97%

Plumb for more details). It has been applied to stratospheric flows and shown to work quite well when the flow is nearly adiabatic-inviscid and, hence, conserves Ertel's PV following air parcels on isentropic surfaces (Waugh 1993a,b; Waugh and Plumb 1994; Waugh et al. 1994). It has also been shown to work reasonably well for periods shorter than 2 weeks or so when applied to upper-tropospheric flows (M. Nakamura 1994).

First, we used the composites of PV_{250} at day -4 to initialize the PV contours in CAS and then advected them by the geostrophic wind derived from composite Z_{250} with the latitude-dependent Coriolis parameter. In a second set of experiments, CAS was initialized with the same PV field, but the advecting geostrophic wind was derived from the hypothetical Z_{250} composites from which the transient feedback had been removed. In practice, the hypothetical composites were obtained by adding $\tilde{Z}^*_{250}$ to the climatological-mean Z_{250}. In all integrations we used 50 time steps per day (i.e., the 12-h wind data were linearly interpolated into 24 time steps between any pair of the adjacent frames) and integrated from day -4 through day $+1$ for each of the eight composite datasets based on E1, P1, E2, and P2: four with the total low-pass-filtered wind and the other four with the low-pass-filtered wind minus the transient eddy contribution. For the sake of easier inspection of the results, we used only three contour lines (1, 2, and 3 PVU) for each experiment. Strictly speaking, PV_{250} is conserved in adiabatic-inviscid flows only following the three-dimensional trajectories. Therefore, the use of PV_{250} and the 250-mb wind in CAS is likely to produce larger errors than the use of Ertel's PV and wind on an isentropic surface. However, vertical velocity is much smaller than the horizontal velocity at the 250-mb level and, hence, we are not seriously concerned with the loss of accuracy due to the use of the isobaric quantities in these short CAS integrations.

The middle columns of Figs. 5 and 6 show evolutions of the PV contours due to advection by the composite low-pass-filtered wind for E1 and P1, respectively. The observed evolutions of the same PV contours based on the low-pass-filtered composites are shown in the left columns of those figures. One can see in Fig. 5 that the overall structure of the blocking observed over Europe is reproduced reasonably well by CAS in which PV was advected by the low-pass-filtered wind. Similarly, there is a reasonable agreement between the CAS-produced (due to the advection by the low-pass-filtered wind) and the observed PV evolution in the composite for the Pacific blocking (Fig. 6). M. Nakamura (1994), who applied CAS to five blocking events simulated in a high-resolution climate GCM and two observed events, found that advection by low-pass-filtered wind accounts for most of the low-frequency PV evolution within those seven events, in agreement with the results found here from the blocking composites.

However, as mentioned earlier, part of the low-pass-filtered wind stems from the forcing by the high-frequency transients. The potential importance of the transient feedback in the evolution of strong blocking events may be examined by comparing the CAS integrations with and without that feedback, shown in the middle and right columns, respectively, of Figs. 5 and 6. For E1, CAS reproduces the broad structure of PV_{250} reasonably well regardless of the presence of the feedback, although there are noticeable differences between the two integrations (Fig. 5). With the transient feedback, a tongue of the low-PV air (between 1 and 2 PVU), which intrudes into the blocking ridge and then wraps up anticyclonically after day -1, is about twice as large as that without the feedback. Moreover, without the feedback, the blocking region as identified in PV_{250} appears to shift downstream slightly (see days 0 and $+1$), consistent with theoretical studies (e.g., Shutts 1983; Haines and Marshall 1987).

In contrast, there are major differences in the PV evolution between the two CAS integrations for P1 (Fig. 6). At day -1, there is already a conspicuous difference in the size of the poleward-intruding low-PV tongue (1–2 PVU). In fact, there is no poleward intrusion of low-PV air at all throughout the integration without the feedback, whereas a large pool of low-PV air is entrained into the blocking in the presence of the feedback. Also, the strong anticyclonic rotation of PV_{250} evolution simulated with the feedback is hardly seen when the feedback was removed.

The same qualitative differences in the potential impact of the transient feedback as mentioned above are observed for E2 and P2 (not shown). CAS reproduces the overall structure of the PV_{250} evolution in the composite for E2 reasonably well, even without the transient feedback. For P2, in contrast, a CAS integration without the feedback again fails to reproduce the poleward intrusion of low-PV air and its anticyclonic evolution. Since CAS does not physically represent diabatic effects in the atmosphere, the results described here are biased toward overestimating the role of advection. However, the neglect of diabatic effects is not likely to severely affect the integrations over relatively short periods at high altitudes, such as those presented here. Although qualitative, these results clearly demonstrate the difference in the potential importance of the transient feedback in the blocking formation between the North Pacific and Europe.

6. Barotropic model experiments

The CAS experiments in the preceding section clearly differentiate two types of blocking formation in the contrasting evolution of PV contours between the two blocking patterns as advected by the hypothetical sequence of wind composites from which the forcing by the high-frequency transient eddies (F_{HFT}) has been removed. Yet one may argue that PV is not merely a passive tracer as treated in the CAS experiments but rather an ''active'' tracer that modifies the ambient flow while advected.

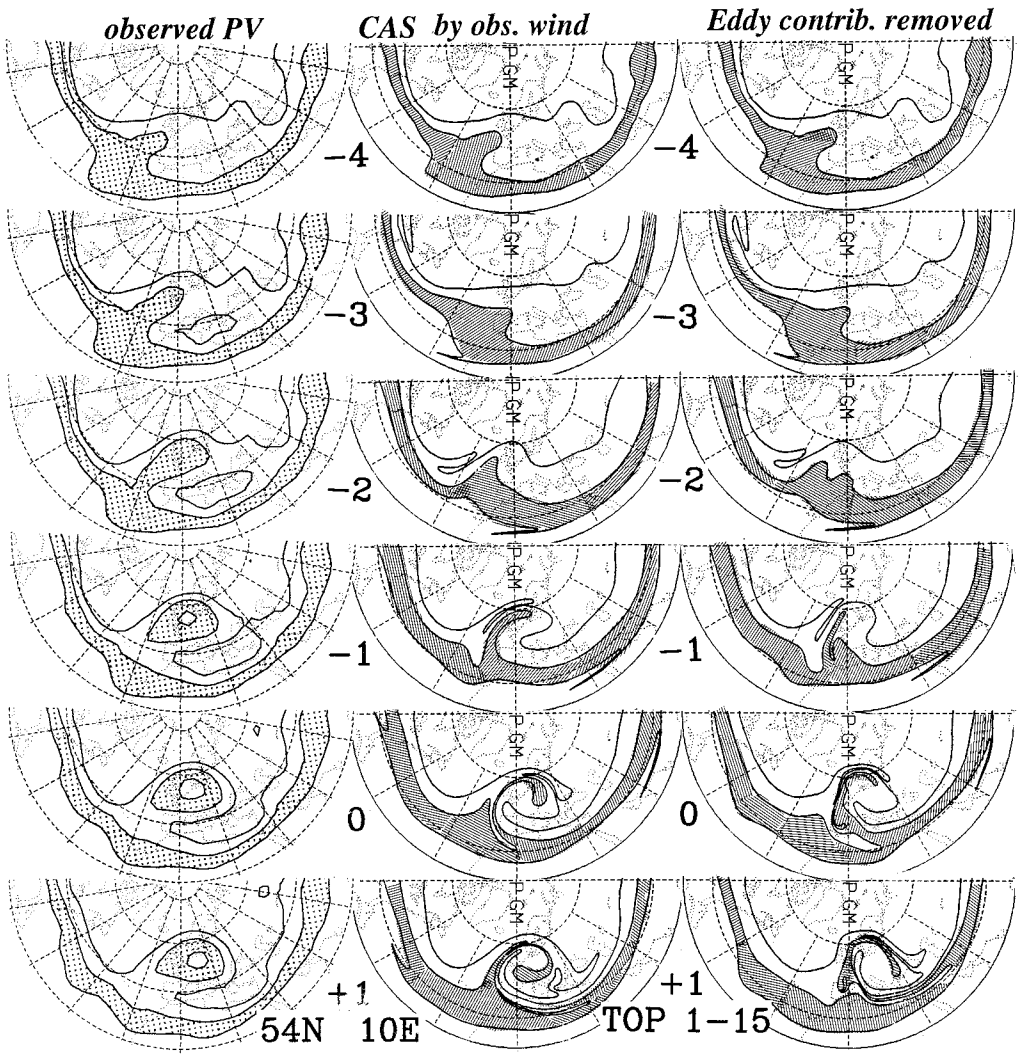

FIG. 5. Evolution of PV_{250} contour lines for 1, 2, and 3 PVU for days relative to the peak time as indicated (negative and positive values signify the amplification and decay stages, respectively), based on the low-pass-filtered PV composite (left; reproduced from Fig. 1) and CAS experiments with low-pass-filtered 250-mb geostrophic wind as observed (middle) and the same wind from which barotropic forcing by high-frequency transients $(\partial Z^*_{250}/\partial t)_{\mathrm{HFT}}\Delta t$ has been subtracted at each time step with half-day lag intervals (i.e., $\Delta t = 0.5$ day) after day −4 (right). The PV_{250} composite for day −4 was used as the initial field for CAS. Composited PV and wind evolutions are based on the 15 strongest blocking events at 54°N, 10°E in the last 27 winter seasons. Shaded where $1 < PV_{250} < 2$ (PVU). In each panel the area 20°–90°N, 90°W–90°E is plotted with the meridian of Greenwich in front.

Furthermore, some uncertainties remain in evaluating the influence of the transient eddy forcing upon the blocking formation. First, part of the barotropic forcing evaluated in this study tends to be canceled by the baroclinic forcing by those eddies. Therefore, the results presented above are apt to overestimate the role of the high-frequency transients and underestimate that of the low-frequency dynamics. Second, in comparing the transient eddy forcing with the observed amplification of the blocking, we implicitly assumed the response of the slowly evolving blocking flow (i.e., the time tendency term in the vorticity equation) to the forcing to be approximated by the forcing pattern itself. Strictly speaking, the forcing and the response should not be identical because part of the forcing must be balanced with the advection by the slowly evolving flow.

In order to clarify those points, the evolution of the composite blocking events was diagnosed using a numerical model of the barotropic vorticity equation on the sphere. A spectral model with a triangular truncation (T42) was used to integrate the equation

$$\frac{\partial}{\partial t}\nabla^2\psi = -J(\psi, \nabla^2\psi + f) - \kappa\nabla^8\psi + F_c + F_{\mathrm{HFT}}. \quad (1)$$

In (1), ψ is the streamfunction, f is the Coriolis parameter, ∇^2 is the horizontal Laplacian on the sphere, J is

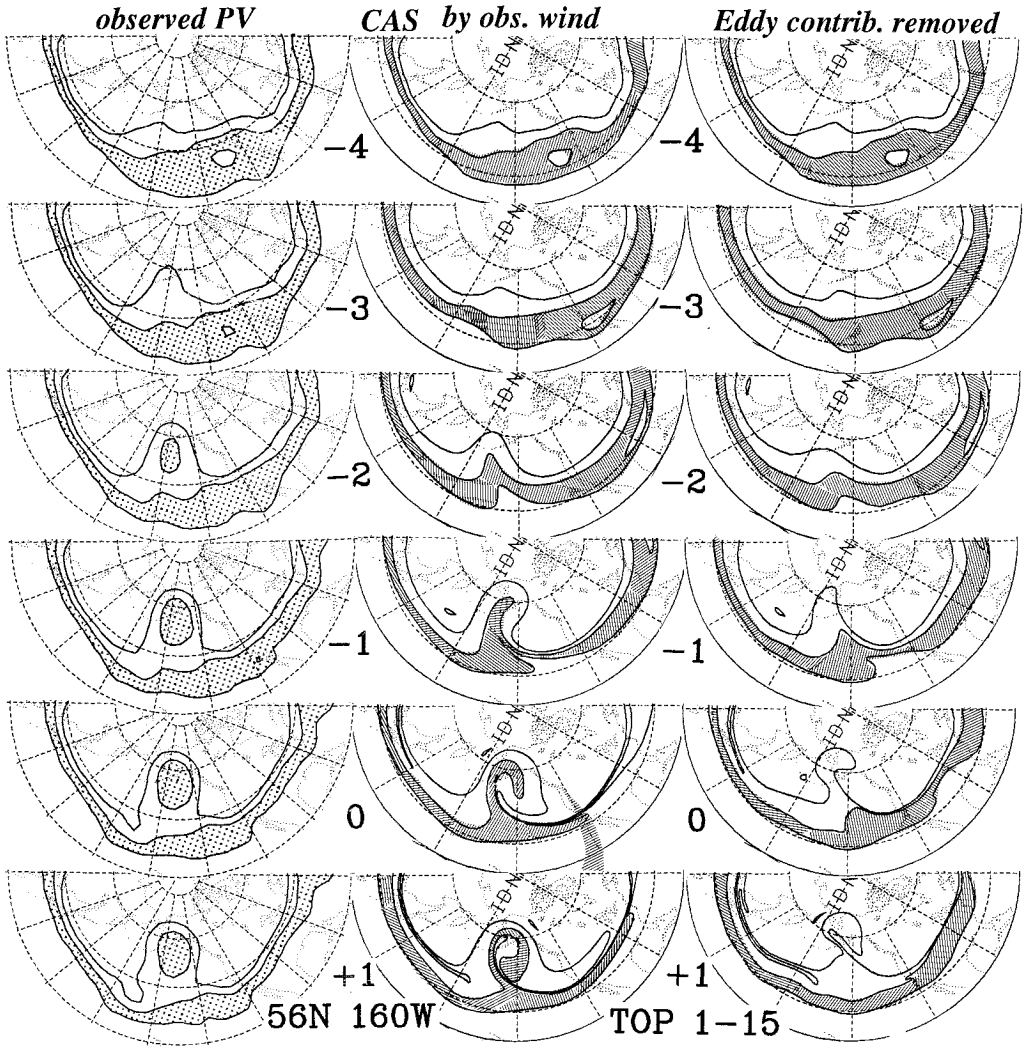

FIG. 6. As in Fig. 5 but for 56°N, 160°W. Composited PV_{250} evolution (left) is reproduced from Fig. 2. In each panel the area 20°–90°N, 120°E–60°W is with 150°W in front.

the spherical Jacobian operator, and κ is the damping strength. Damping strength κ is selected so that the smallest resolved wave is damped with a 1-day timescale, though results were qualitatively insensitive to this value. The climatological forcing F_c is chosen so that the wintertime climatological-mean streamfunction at 250 mb ψ_c is a stationary solution of (1):

$$F_c = J(\psi_c, \nabla^2\psi_c + f) + \kappa\nabla^8\psi_c, \qquad (2)$$

when the term F_{HFT} is neglected. This climatological forcing is the same as that hypothesized to exist in the computation of unstable normal modes of zonally varying flows (Simmons et al. 1983). It has long been known (Wolff 1958) that barotropic models such as (1) without some sort of climatological forcing produce unrealistic rapidly retrogressing long waves and a somewhat less rapid loss of amplitude in all waves. As in the instability problems, the introduction of the forcing here is a simple means of parameterizing the time-mean impact of any number of processes not resolved in the barotropic model.

The forcing effects of the high-frequency transient eddies are represented by F_{HFT}. Composite means of the instantaneous time tendency of 250-mb relative vorticity due to those eddies were produced by evaluating $\nabla^2(\partial Z^*_{250}/\partial t)_{\mathrm{HFT}}$ at 12-h intervals for periods surrounding the peak blocking time. At each time step of the barotropic model, a linear interpolation into this time series of composite transient forcing was used to obtain the instantaneous time tendency of vorticity from the transient eddies.

The barotropic model was integrated starting from initial conditions ranging from 4 to 0 days before the peak blocking time. As an example of the results, Figs. 7 and 8 show the evolution of the streamfunction for integrations started from initial conditions 3 days before the peak time for E1 and P1, respectively. The corre-

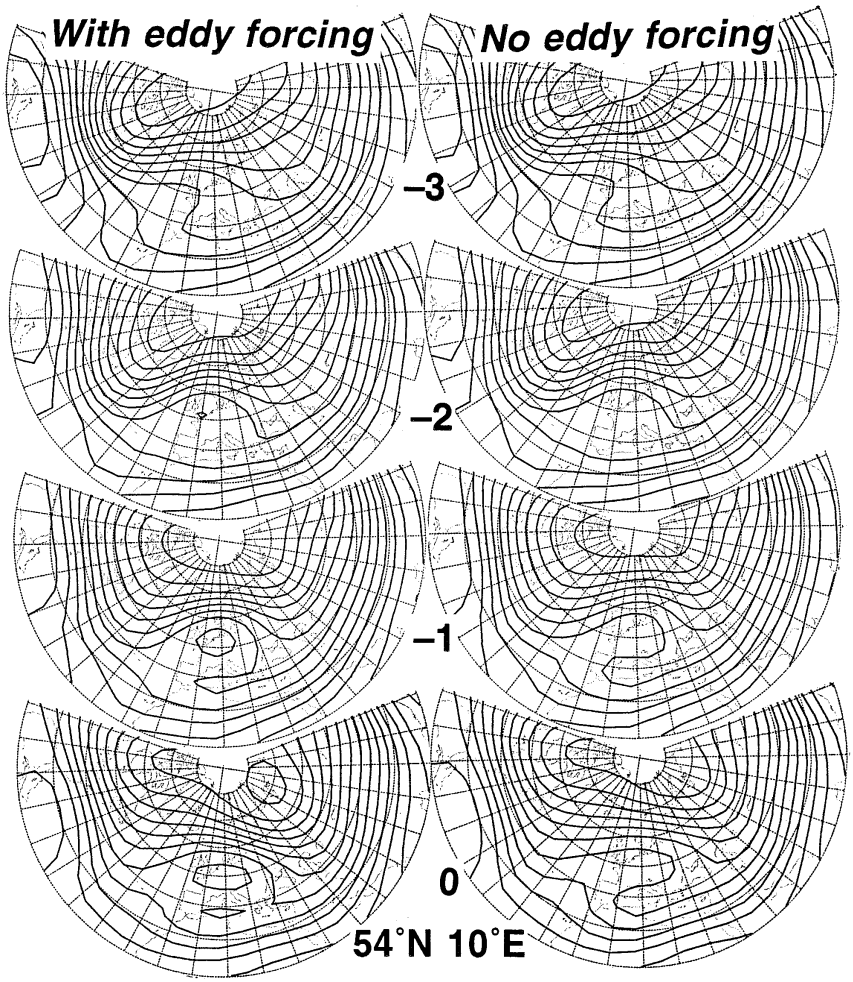

FIG. 7. Evolution of 250-mb streamfunction (every 10^7 m^2 s^{-1} $\approx$ 100 m in Z_{250}) for days relative to the peak time as indicated (negative and positive values signify the amplification and decay stages, respectively), simulated in barotropic model integrations in which observed barotropic forcing by high-frequency transient eddies $(\partial Z^*_{250}/\partial t)_{\mathrm{HFT}}$ was imposed at every time step (left) and no such forcing was imposed (right). The model was initialized with Z_{250} composite for day -3 based on the 15 strongest blocking events at 54°N, 10°E. In each panel the area 20°–90°N, 100°W–120°E is plotted with 10°E in front.

sponding evolution of the streamfunction anomaly is shown in Figs. 9 and 10. In each of the figures, the right column is from integrations in which the high-frequency forcing term F_{HFT} was not included, while the left column includes this term. In any of the integrations, the blocking tends to grow and decay somewhat faster than in the real atmosphere. Therefore, the peak time of the simulated blocking is somewhere between days -1 and 0. Still, in both regions, a significant blocking development takes place during the first 3 days of the barotropic model integration when the forcing from the transient eddies is included. However, when this forcing is excluded, the Pacific block fails to develop significant strength, although the European block continues to demonstrate nearly as much development as in the forced case. For example, the difference in the maximum anticyclonic streamfunction anomaly for the Pacific blocking between the integrations with and without the transient forcing is twice as strong as that for the European blocking (Figs. 9 and 10). Table 2 shows a measure of blocking strength for each of the four barotropic model integrations. The blocking index of Anderson (1993) is a function of longitude and measures the largest difference in streamfunction between pairs of grid points at different latitudes between 35° and 70°N but at the same longitude. The index is positive when streamfunction increases with latitude in the presence of the easterlies. The table displays the largest value of the blocking index, converted to geopotential height difference, for longitudes within 15° of the center of the composite blocks. In other words, the table shows the index measured as the geopotential height difference

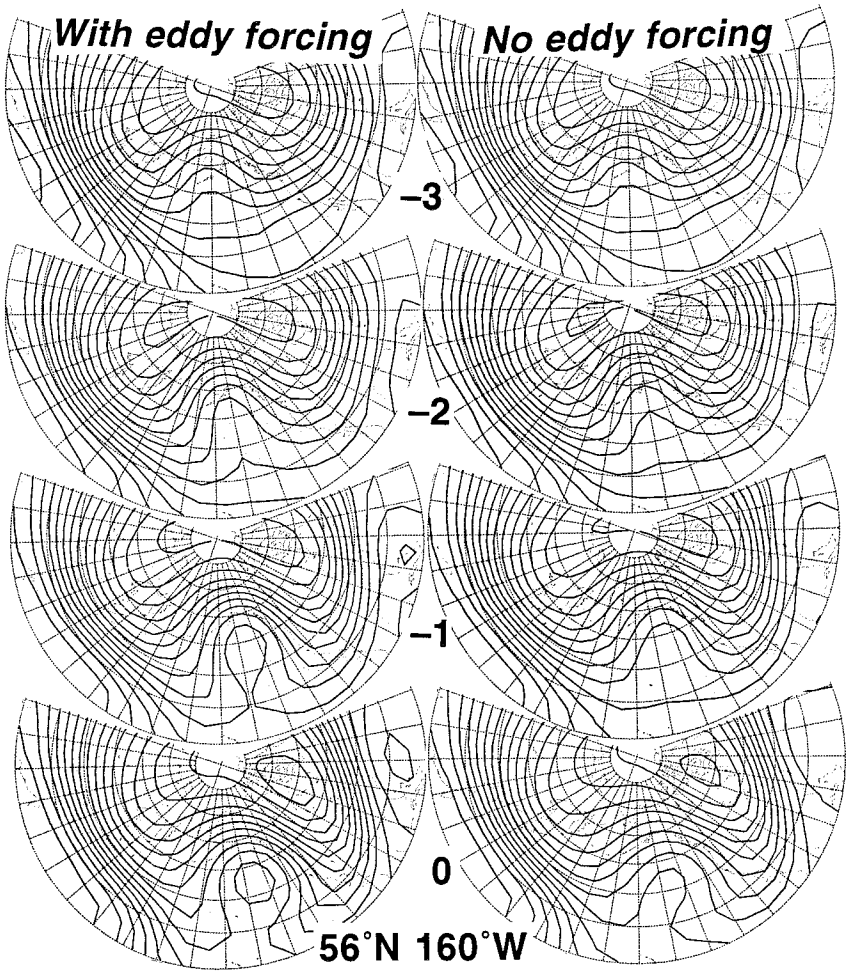

FIG. 8. As in Fig. 7 but for 56°N, 160°W. In each panel the area 20°–90°N, 90°E–50°W is plotted with 160°W in front.

between the anticyclonic center of a blocking ridge and the center of the nearest midlatitude trough to the south along a particular meridian. Table 2 highlights the relative lack of importance of the transient forcing upon the blocking development over Europe and the lack of blocking development in the Pacific without that forcing. The index values for the blocks simulated with the transient forcing are in the same order of magnitude as those for the observed blocks. This result indicates that the model with the transient forcing reproduced the observed blocks reasonably well, although the simulated Pacific block is somewhat too strong.

Results for barotropic integrations from the composite streamfunction for other lags before the peak blocking time also showed blocking development. However, initial conditions from 2 days or less before the peak time are already quite strongly blocked, so relatively little additional blocking development can occur during ensuing days. Integrations started from 4 days before the peak time lead to some blocking development in the barotropic integrations; however, the strengthening is considerably less in all cases than in the 3-day precursor cases discussed in detail above. The impact of the transient forcing for both the 2- and 4-day precursor integrations is qualitatively consistent with the 3-day precursor results.

Other aspects of the development of the composite blocks in the barotropic model integrations are also consistent with the observations and the CAS results in section 5. For instance, the European block clearly shows an anticyclonic rotation of the streamfunction and vorticity fields as the block strengthens. Integrations for the Pacific blocking do not show nearly as much evidence of ''rotation,'' although there are hints that a cyclonic rotation is occurring during the blocking development.

The barotropic model integrations were also performed for the composites E2 and P2. In these cases, the development of blocking was found to be significantly less for all initial condition lags for the two regions. The impact of the high-frequency transients, especially in the Pacific case, became even more significant to the development of blocking in these inte-

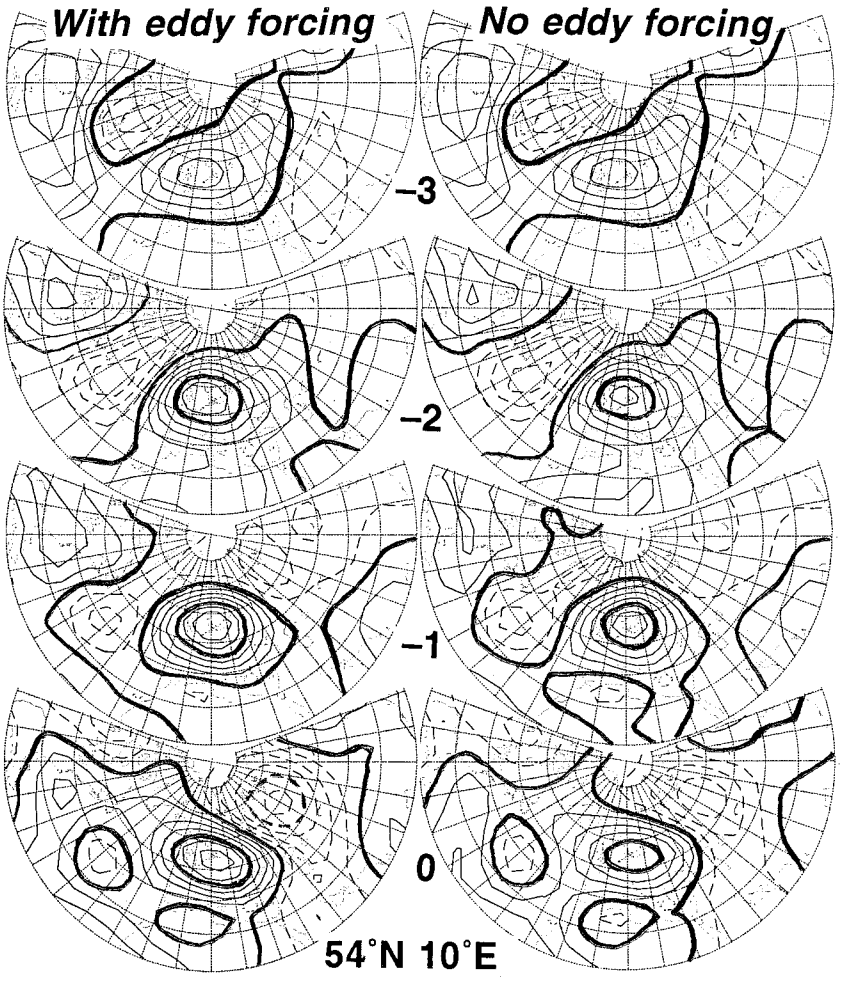

FIG. 9. As in Fig. 7 but for 250-mb streamfunction anomalies in the model integrations for 54°N, 10°E (every 5×10^6 m^2 s^{-1} $\approx$ 50 m in Z_{250} anomaly; thickened for every 2×10^7 m^2 s^{-1}). In each panel the area 20°–90°N, 100°W–120°E is plotted with 10°E in front.

grations. In fact, the observational analysis shows that the transients contribute more to the development of P2 than to the development of any other blocking cases examined in section 4 (Table 1).

7. Transient feedback during the blocking decay

Thus far we have examined the role of the feedback from high-frequency transients and low-frequency dynamics such as quasi-stationary Rossby waves in the formation of strong blocking anticyclones. In this section, we will summarize their role in the breakdown of the blocking. Comparison of the anomalous VH_{250} (left columns) composites between days 0 and +3 in Figs. 1 and 2 reveals that the anomalous transient eddy activity tends to be distributed in the same manner throughout the mature and decay stages of the blocking, although the anomalous activity gradually weakens. Consistent with this result, the high-frequency transient eddies still impose significant anticyclonic forcing, that is, positive $(\partial Z^*_{250}/\partial t)_{\text{HFT}}$, upon the anticyclonic anomalies in low-pass-filtered Z_{250} in the decay stage, as they do in the amplification and mature stages (Figs. 3 and 4). A more quantitative evaluation is given in Table 3, where $(\partial Z^*_{250}/\partial t)_{\text{HFT}}$ accumulated from day 0 to day +4 in the vicinity of the blocking anticyclone center is compared with the change in the strength of the blocking anomaly observed in the low-pass-filtered Z_{250} during the same 4-day period. These procedures are essentially the same as used for Table 1. As in the amplification stage, anticyclonic forcing by the high-frequency transients reinforces the existing anticyclonic anomalies. Unlike in the amplification stage, however, the forcing turns out to be against the tendency in the low-frequency field associated with the decaying ridges. The stronger initial decay of the blocking in the barotropic model integrations without the transient forcing than in those with the forcing confirms that the transient eddies counteract the breakdown of the blocking (Figs. 9 and 10). Therefore, the breakdown of the blocking should be

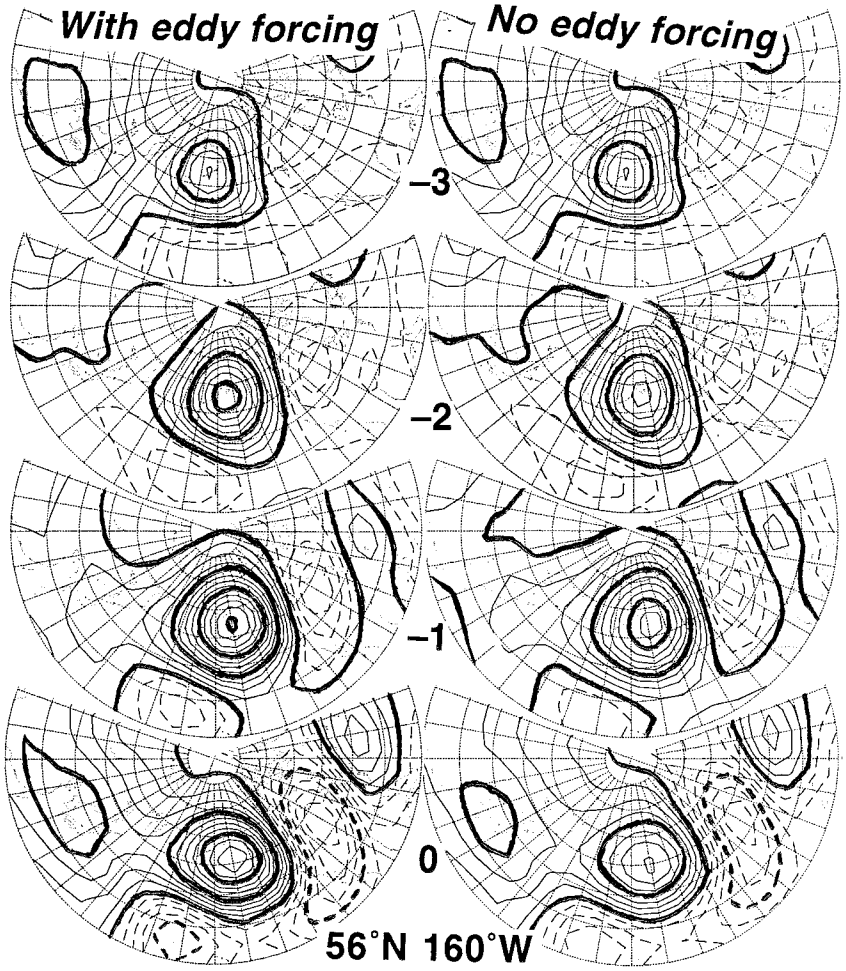

FIG. 10. As in Fig. 9 but for 56°N, 160°W. In each panel the area 20°–90°N, 90°E–50°W is plotted with 160°W in front.

TABLE 2. Strength of Anderson's (1993) blocking index as a function of time relative to the peak blocking time (in days, first column) for barotropic model integrations with initial conditions taken from composites for 3 days before the peak blocking time. The composite is based on the 15 strongest blocking events at each of the locations as listed. The index values, represented as the maximum geopotential height (m) at the center of a blocking ridge minus the minimum height (m) at the nearest midlatitude trough to the south, are listed separately for the integrations with (yes) and without (no) the barotropic forcing by the high-frequency transient eddies. The index values based on the observed blocking composites at day 0 are also listed.

Transient forcing	54°N, 10°E		56°N, 160°W	
	Yes	No	Yes	No
Day −3	28.5	28.5	−109	−10.9
Day −2	65.2	43.1	−0.1	−10.5
Day −1	165	108	94	12.8
Day 0	159	112	204	59.6
Observation	184		120	

attributed to the low-frequency dynamics, more specifically, the downstream emanation of a quasi-stationary Rossby wave train from a blocking ridge, as pointed out by Dole (1983, 1986, 1989) and Black (1997).

It may be noteworthy that for the blocking over Europe $\Delta Z^*_{\mathrm{HFT}}$ in the decay stage is substantially stronger than in the amplification stage, whereas the opposite is the case for the blocking over the North Pacific (Tables 1 and 3). Presumably, a blocking ridge over Europe initially amplifies due to the wave activity flux convergence at the downstream end of a quasi-stationary Rossby wave train across the North Atlantic. Then, after the blocking ridge reaches certain strength, the migratory eddies along the northward-shifted local storm track start imposing significant anticyclonic forcing on the ridge. Over the North Pacific, in contrast, the anomalously enhanced activity of those eddies and their strong anticyclonic forcing are perhaps necessary even for the initial amplification of the blocking.

TABLE 3. As in Table 1 but for the blocking breakdown (from day 0 to day +4).

	Amplitude rank	Z^* (m) peak	Z^* (m) day +4	ΔZ^* (m) obs.	HFT forcing (m)	HFT contribution
54°N, 10°E	1–15	287	88	−199	124	−63%
(Europe)	16–30	259	127	−132	81	−62%
56°N, 160°W	1–15	411	231	−180	126	−70%
(North Pacific)	16–30	338	141	−197	86	−43%

8. Summary and discussion

The composite time evolution of the 30 strongest blocking episodes observed over Europe and the North Pacific suggests that the mechanism for the blocking formation substantially differs between the two locations. Over Europe the transient eddy feedback accounts for less than 45% of the actual amplification of the blocking. The major portion of the formation should be attributed to the low-frequency dynamics in the form of the convergence (or absorption) of wave activity density flux associated with an incoming quasi-stationary Rossby wave train. In contrast, the low-frequency dynamics only plays a secondary role in the formation of strong blocking ridges over the North Pacific. Transient eddies that have grown in the Pacific storm track impose a strong positive feedback upon the blocking, which accounts for more than 75% of the observed amplification of the blocking. The observed distinction in the blocking formation between these locations can be demonstrated in a pair of the CAS experiments, one in which given PV contours were advected with the low-pass-filtered composite sequence of the observed wind, and the other in which the observed barotropic forcing by the transient eddies had been removed from the composite sequence. The low-frequency dynamics should be a dominant contributor to the time evolution in the wind field used in the latter experiment. In the CAS experiments for the European blocking, the observed intrusion of low-PV air from the subtropics into higher latitudes and subsequent anticyclonic evolution of the low-PV center were reproduced, with or without the transient feedback. However, the intrusion cannot be reproduced without the transient forcing in the experiments for the North Pacific. Thus, the CAS experiments give certain confirmation to the observational results. We also performed a pair of barotropic model integrations that were started with the identical initial condition based on the low-pass-filtered composites, one in which the observed barotropic forcing by the transient eddies was continuously imposed and the other in which it was not. These integrations revealed that the inclusion of the transient forcing added greater positive contributions to the blocking formation over the Pacific than over Europe, which is consistent with the observed findings and the CAS results.

The results in the present study are in good agreement with the recent studies by H. Nakamura (1994) and M. Nakamura (1994), in which the importance of the low-frequency dynamics in the blocking formation was suggested. The wave activity propagation through a quasi-stationary Rossby wave train across the North Atlantic appears to be obstructed temporarily in the weak-westerly domain associated with an incipient blocking ridge over Europe, which probably leads to the ensuing enhancement of the ridge. As the low-PV center evolves anticyclonically within the blocking ridge, the correlation between the meridional wind velocity and PV changed from negative to positive. In the light of the flux divergence of wave activity density, this change is consistent with an incoming Rossby wave train in the amplification stage and the subsequent emanation of another wave train from the decaying ridge. The anticyclonic PV evolution resembles the nonlinear Rossby wave breaking found in numerical simulations (Haynes and McIntyre 1987; Held and Phillips 1990; Nakamura and Plumb 1994). M. Nakamura (1994) showed through his CAS experiments that the incoming Rossby wave train indeed broke over Europe as a strong blocking ridge formed and then decayed. He also showed that the formation of GCM-simulated Southern Hemisphere blocking was accompanied by Rossby wave breaking. It should be stressed that the presence of a Rossby wave train itself does *not* characterize the blocking. Furthermore, our results do *not* suggest that the blocking formation is attributed to the linear dynamics associated with Rossby wave propagation, that is, within the framework of the nonacceleration theorem. Rather, we *do* suggest that the breakdown of the nonacceleration theorem by the temporary obstruction of wave propagation associated with wave breaking and the subsequent saturation processes may explain the time evolution of the strong blocking observed over Europe. Our results are consistent with the fact that blocking of the westerly flow was simulated even in barotropic models (e.g., Legras and Ghil 1985).

Although the low-frequency dynamics was found to be a primary contributor to the formation of strong blocking ridges over Europe, the positive feedback from the high-frequency transient eddies cannot be totally neglected. The feedback forcing is indeed of secondary importance but not negligible, particularly for the 15 strongest blocking events. The strength of the transient forcing may be one of the factors that determine whether an amplifying block over Europe becomes one of the 15 strongest (Table 1) or whether it ends up with a somewhat weaker one (Table 1), although the 15 strongest events also tend to exhibit stronger obstruction of the Rossby wave propagation than the weaker events

do (H. Nakamura 1994). Furthermore, if the blocking formation is concomitant with an incoming Rossby wave train from upstream, the high-frequency transients impose positive feedback not only upon anticyclonic anomalies that later form into a blocking ridge but also upon other anomalies associated with the wave train. In fact, the cyclonic anomalies observed over the North Atlantic during the amplification stage of the European blocking became significantly weaker when the transient forcing was removed (Fig. 3). Presumably, the forcing the transient eddies impose along the Rossby wave train is transferred downstream by the wave activity density flux and then deposited into the amplifying blocking ridge. Moreover, a wave train as observed upstream of a blocking ridge might be generated in response to the local forcing imposed farther upstream by transient eddies. Our observational analysis and CAS experiments cannot isolate such indirect feedback forcing by the transients upon the low-frequency circulation anomalies.

Results of the present study indicate that a classic picture of the blocking formation due mainly to the feedback from the high-frequency transients is still valid in the vicinity of the Pacific storm track. M. Nakamura (1994), who applied CAS to a strong blocking event over the North Pacific, found that PV advection by the high-pass-filtered flow is important during the first 5 or 6 days of the event. He speculated that it was initiated by the sudden obstruction of the zonal flow by strong diffluence due to ''explosive'' cyclogenesis, which is reinforced by successive incoming synoptic-scale eddies. It may be such sudden and strong conversion of potential energy of the transient eddies to kinetic energy that produces the large low-frequency height tendency found in the blocking composite for the North Pacific. This speculation is consistent with the observational fact that the blocking formation over the North Pacific is associated with strong anticyclonic forcing by the transient eddies (Figs. 2 and 4). Yet the transient forcing cannot entirely explain the observed rate of the blocking amplification over that region, especially for the 15 strongest events. Some kind of low-frequency dynamics must play a nonnegligible, secondary role in the amplification (Table 1). It may also be the case even for weaker events, since the transient feedback evaluated solely by the barotropic component should be overestimated. Black (1997) found that persistent anticyclonic anomalies over the North Pacific are associated with the upward flux of wave activity density converging into the upper troposphere. This convergence appears to act as the primary source of the flux emanating downstream in the upper troposphere. The barotropic feedback from the high-frequency transients probably accounts for most of the net divergence of that flux in the upper troposphere. It is unlikely, however, that the barotropic feedback, which is substantially weaker in the lower troposphere than aloft, acts as the primary source of the upward flux. The anomalous divergence of the low-level heat fluxes associated with the high-frequency transients may contribute to the generation of that upward flux to some extent. The large-scale baroclinic processes in the lower troposphere associated with the quasi-stationary flow anomalies over the North Pacific may also contribute (Black and Dole 1993).

Comparison between our results for the European blocking and the case studies by Shutts (1986) and Chen and Juang (1992) indicates that the importance of the low-frequency dynamics in the blocking formation might depend rather sensitively upon the exact location of a blocking pattern. The blocking anticyclones they analyzed are located some 1500 km northwest and north of our European blocking pattern, respectively. They argued that the feedback from the transient eddies plays an important role in the formation of those blocks, although the slow, steady anticyclonic evolution of the low-PV center can be seen, particularly in the analysis by Shutts. Generalization of the findings in the present study is under way by applying the same kind of analyses to the composite time evolution of the strongest blocking events observed at each of a number of grid points in the extratropical Northern Hemisphere. A preliminary result indicates that the transient eddies tend to exert stronger feedback during the blocking formation that occurs farther to the north or west of our European blocking pattern.

Acknowledgments. We thank Dr. Darryn Waugh for kindly giving us his CAS code. We also thank Dr. N.-C. Lau for his valuable comments on the first draft of this paper. One of the authors (MN) is partially supported by NOAA Grant NA90AA-D-AC513.

APPENDIX A

A Measure of Amplitude Modulation of Transient Eddies

In order to examine how the amplitude (or activity) of the high-frequency transient eddies is modulated as a blocking ridge evolves, we need to define their instantaneous amplitude at a particular location. The 8-day low-pass-filtered wind was regarded as the basic flow upon which the eddies are superimposed. Gradual evolution of the basic flow is accompanied by amplitude modulation of the eddies that are baroclinic disturbances propagating along the jet streams. Since they are, in general, elongated in the direction perpendicular to the local jet axis [as represented by the eastward-pointing extended E–P flux vectors along the storm tracks; see Hoskins et al. (1983)], wind fluctuations associated with the eddies are projected mainly onto that direction. Furthermore, the background flow as defined above evolves so slowly that the unfiltered wind component perpendicular to the background flow (V_{PJ}) is associated mostly with those eddies. Since V_{PJ} fluctuates between positive (northward) and negative (southward) values as the eddies pass by, their instantaneous amplitude at a given location may be measured as

$$\mathrm{VH} = (2\overline{V_{PJ}^2})^{1/2},$$

where the overbar denotes the 8-day low-pass filtering. If the background wind speed is less than 0.5 m s^{-1}, VH was set to be zero because the direction of the background flow is poorly defined. Justification may be given by the tendency that the baroclinic eddies are very weak where the background westerlies are weak. We evaluated VH based on Z_{250}, assuming geostrophic balance with the latitude-dependent Coriolis parameter. As VH itself is a low-pass-filtered quantity, its climatological-mean seasonal cycle was obtained in the same manner as in section 2. Here VH is an alternative measure of instantaneous amplitude of the high-frequency transients to the ''envelope function'' used by Nakamura and Wallace (1990). In fact, the climatological-mean distribution of VH for each month is very similar to that of the envelope function. Note that, unlike the envelope function, VH is not based on explicit high-pass filtering and cannot be well defined in the lower troposphere where the background flow is very weak.

APPENDIX B

A Measure of Barotropic Feedback from Transient Eddies

In the present study, the barotropic feedback has been evaluated as the low-pass-filtered tendency of the 250-mb geopotential height due solely to the vorticity flux convergence associated with the high-frequency transients at that level, that is,

$$\left(\frac{\partial Z_{250}}{\partial t}\right)_{\text{HFT}} = \frac{f_0}{g}\nabla^{-2}[-\nabla\cdot(\overline{v'\zeta'} + \overline{\bar{v}\zeta'} + \overline{v'\bar{\zeta}})], \quad \text{(B1)}$$

where overbars and primes denote the 8-day low-pass- and high-pass-filtered quantities, respectively; f_0 is the Coriolis parameter at 43°N ($=1 \times 10^{-4}$ s^{-1}); g is the acceleration of gravity; v is the horizontal wind; and ζ is the relative vorticity. The high-pass-filtered quantities were obtained by subtracting the low-pass-filtered quantities from the unfiltered ones. In solving Poisson's equation (B1), $(\partial Z_{250}/\partial t)_{\text{HFT}} = 0$ was imposed along the boundary (south of 17°N) of the NMC octagonal grid, a 1977-point square grid system on a polar stereographic projection. This rather artificial boundary condition is not expected to cause any serious error in the solution of (B1) because baroclinic eddies are generally very weak in the subtropics. Since f_0 is fixed to the value of 43°N, (B1) yields a streamfunction tendency, which can be compared with the observed streamfunction-like height anomalies. Twice-daily fields of the NMC 250-mb horizontal wind were used for computing the vorticity fluxes on the right-hand side of (B1). If the wind field is missing while Z_{250} is available, the geostrophic wind field based on Z_{250} (with latitude-dependent f) was substituted into the sequence of the wind fields. If both of the variables are missing, the missing wind field was filled by linear interpolation in time. Since the cutoff of the filter response function is not as sharp as the step function, the resultant imperfect separation between the high-pass- and low-pass-filtered quantities yields some values in the second and third terms (i.e., ''cross terms'') of (B1). Still, the first term was found to dominate the other two. Compared to an evaluation of the net feedback by solving the three-dimensional Poisson's equation, the evaluation with (B1) applied only to the 250-mb surface can reduce the computational burden by one order of magnitude, and therefore the feedback could be evaluated twice every day over the 27-yr period.

Based on the low-pass-filtered flux convergence, $(\partial Z_{250}/\partial t)_{\text{HFT}}$ itself is a slowly varying quantity, too. The 31-day moving average of $(\partial Z_{250}/\partial t)_{\text{HFT}}$ was used to obtain the mean annual cycle for the 27-yr period. The wintertime climatological mean resembles the results by Lau and Holopainen (1984). The climatological-mean feedback from the transient eddies should be balanced by other dynamical processes such as the horizontal advection of the absolute vorticity and the vortex-tube stretching associated with the horizontal divergence. Therefore, the effective feedback upon the low-frequency circulation anomalies such as blocking ridges should be given by $(\partial Z^*_{250}/\partial t)_{\text{HFT}}$, the anomalous $(\partial Z_{250}/\partial t)_{\text{HFT}}$, defined as the departure from its climatological-mean annual cycle. The feedback was evaluated in a similar manner in Nakamura (1990). Compared to the present study, however, the feedback was somewhat underestimated in his study because the cutoff period of the filter was set to 6 days rather than 8 days and no cross terms were included.

REFERENCES

Anderson, J. L., 1993: The climatology of blocking in a numerical forecast model. *J. Climate,* **6,** 1041–1056.

Berggren, R., B. Bolin, and C.-G. Rossby, 1949: An aerological study of zonal motion, its perturbations and break-down. *Tellus,* **1,** 14–37.

Black, R. X., 1997: Deducing anomalous wave source regions during the life cycles of persistent flow anomalies. *J. Atmos. Sci.,* **54,** 895–907.

——, and R. M. Dole, 1993: The dynamics of large-scale cyclogenesis over the North Pacific Ocean. *J. Atmos. Sci.,* **50,** 421–442.

Blackmon, M. L., S. L. Mullen, and G. T. Bates, 1986: The climatology of blocking events in a perpetual January simulation of a spectral general circulation model. *J. Atmos. Sci.,* **43,** 1379–1405.

Branstator, G., 1992: The maintenance of low-frequency atmospheric anomalies. *J. Atmos. Sci.,* **49,** 1924–1945.

Chen, W. Y., and H.-M. H. Juang, 1992: Effects of transient eddies on blocking flows: General circulation model experiments. *Mon. Wea. Rev.,* **120,** 787–801.

Colucci, S. J., 1985: Explosive cyclogenesis and large-scale circulation changes: Implications for atmospheric blocking. *J. Atmos. Sci.,* **42,** 2701–2717.

——, 1987: Comparative diagnosis of blocking versus nonblocking planetary-scale circulation changes during the synoptic-scale cyclogenesis. *J. Atmos. Sci.,* **44,** 124–139.

Crum, F. X., and D. E. Stevens, 1988: A case study of atmospheric blocking using isentropic analysis. *Mon. Wea. Rev.,* **116,** 223–241.

Dole, R. M., 1983: Persistent anomalies of the extratropical Northern Hemisphere wintertime circulation. *Large-Scale Dynamical Pro-*

cesses in the Atmosphere, B. J. Hoskins and R. P. Pearce, Eds., Academic Press, 95–109.

——, 1986: The life cycles of persistent anomalies and blocking over the North Pacific. *Advances in Geophysics*, Vol. 29, Academic Press, 31–69.

——, 1989: Life cycles of persistent anomalies. Part I: Evolution of 500 mb height fields. *Mon. Wea. Rev.*, **117,** 177–221.

Green, J. S. A., 1977: The weather during July 1976: Some dynamical considerations of the drought. *Weather*, **32,** 120–128.

Haines, K., and J. Marshall, 1987: Eddy-forced coherent structures as a prototype of atmospheric blocking. *Quart. J. Roy. Meteor. Soc.*, **113,** 681–709.

Haynes, P. H., and M. E. McIntyre, 1987: On the representation of Rossby wave critical layers and wave breaking in zonally truncated models. *J. Atmos. Sci.*, **44,** 2359–2382.

Held, I. M., and P. J. Phillips, 1990: A barotropic model of the interaction between the Hadley cell and a Rossby wave. *J. Atmos. Sci.*, **47,** 856–869.

Higgins, R. W., and S. D. Schubert, 1994: Simulated life cycles of persistent anticyclonic anomalies over the North Pacific: Role of synoptic-scale eddies. *J. Atmos. Sci.*, **51,** 3238–3260.

Holopainen, E. O., and C. Fortelius, 1987: High-frequency transient eddies and blocking. *J. Atmos. Sci.*, **44,** 1632–1645.

Hoskins, B. J., I. N. James, and G. H. White, 1983: The shape, propagation and mean-flow interaction of large-scale weather systems. *J. Atmos. Sci.*, **40,** 1595–1612.

——, M. E. McIntyre, and A. W. Robertson, 1985: On the use and significance of isentropic potential-vorticity maps. *Quart. J. Roy. Meteor. Soc.*, **111,** 877–946.

Illari, L., and J. C. Marshall, 1983: On the interpretation of eddy fluxes during a blocking episode. *J. Atmos. Sci.*, **40,** 2232–2242.

Kaylor, R. E., 1977: Filtering and decimation of digital time series. Tech. Note BN 850, 42 pp. [Available from Institute for Physical Science and Technology, University of Maryland, College Park, MD 20742.]

Kimoto, M., H. Mukougawa, and S. Yoden, 1992: Medium-range forecast skill variation and blocking transition: A case study. *Mon. Wea. Rev.*, **120,** 1616–1627.

Konrad, C. E., II, and S. J. Colucci, 1988: Synoptic climatology of large-scale circulation changes during explosive cyclogenesis. *Mon. Wea. Rev.*, **116,** 1431–1443.

Lau, N.-C., and E. O. Holopainen, 1984: Transient eddy forcing of the time-mean flow as identified by quasi-geostrophic tendencies. *J. Atmos. Sci.*, **41,** 313–328.

——, and M. J. Nath, 1991: Variability of the baroclinic and barotropic transient eddy forcing associated with monthly changes in the midlatitude storm tracks. *J. Atmos. Sci.*, **48,** 2589–2613.

Legras, B., and M. Ghil, 1985: Persistent anomalies, blocking, and variations in atmospheric predictability. *J. Atmos. Sci.*, **42,** 433–471.

Mak, M., 1991: Dynamics of an atmospheric blocking as deduced from its local energetics. *Quart. J. Roy. Meteor. Soc.*, **117,** 477–493.

Metz, W., 1986: Transient cyclone-scale vorticity forcing of blocking highs. *J. Atmos. Sci.*, **43,** 1467–1483.

Mullen, S. L., 1987: Transient eddy forcing of blocking flows. *J. Atmos. Sci.*, **44,** 3–22.

Nakamura, H., 1990: Observed changes in the activity of baroclinic waves and their feedbacks during the life cycles of the low-frequency circulation anomalies in the Northern Hemisphere winter. Ph.D. dissertation, University of Washington, 248 pp. [Available from Dept. of Atmospheric Sciences, AK-40, University of Washington, Seattle, WA 98195.]

——, 1994: Rotational evolution of potential vorticity associated with a strong blocking flow configuration over Europe. *Geophys. Res. Lett.*, **21,** 2003–2006.

——, and J. M. Wallace, 1990: Observed changes in the baroclinic wave activity during the life cycles of low-frequency circulation anomalies. *J. Atmos. Sci.*, **47,** 1100–1116.

——, and ——, 1993: Synoptic behavior of baroclinic eddies during the blocking onset. *Mon. Wea. Rev.*, **121,** 1892–1903.

Nakamura, M., 1994: Characteristics of potential vorticity mixing by breaking Rossby waves in the vicinity of a jet. Ph.D. dissertation, Massachusetts Institute of Technology, 253 pp. [Available from Department of Earth, Atmospheric and Planetary Sciences, Massachusetts Institute of Technology, Cambridge, MA 02139.]

——, and R. A. Plumb, 1994: The effects of flow asymmetry on the direction of Rossby wave breaking. *J. Atmos. Sci.*, **51,** 2031–2045.

Neilley, P. P., 1990: Interactions between synoptic-scale eddies and the large-scale flow during the life cycles of persistent flow anomalies. Ph.D. dissertation, Massachusetts Institute of Technology, 272 pp. [Available from Department of Earth, Atmospheric and Planetary Sciences, Massachusetts Institute of Technology, Cambridge, MA 02139.]

Plumb, R. A., 1986: Three-dimensional propagation of transient quasi-geostrophic eddies and its relationship with eddy forcing of the time-mean flow. *J. Atmos. Sci.*, **43,** 1657–1678.

Rex, D. F., 1950: Blocking action in the middle troposphere and its effect upon regional climate: I. An aerological study of blocking action. *Tellus*, **2,** 196–211.

Shutts, G. J., 1983: The propagation of eddies in diffluent jetstreams: Eddy vorticity forcing of blocking flow fields. *Quart. J. Roy. Meteor. Soc.*, **109,** 737–761.

——, 1986: A case study of eddy forcing during an Atlantic blocking episode. *Advances in Geophysics*, Vol. 29, Academic Press, 135–162.

Simmons, A. J., J. M. Wallace, and G. Branstator, 1983: Barotropic wave propagation and instability and atmospheric teleconnection patterns. *J. Atmos. Sci.*, **40,** 1363–1392.

Stewart, D. A., 1993: Persistent anomaly forcing in a two-level global circulation model. *J. Atmos. Sci.*, **50,** 2710–2730.

Trenberth, K. E., 1986: An assessment of the impact of transient eddies on the zonal flow during a blocking episode using localized Eliassen–Palm flux diagnostics. *J. Atmos. Sci.*, **43,** 2070–2087.

——, and J. G. Olson, 1988: Evaluation of NMC global analyses: 1979–1987. NCAR Tech. Note TN-299+STR, 82 pp. [Available from National Center for Atmospheric Research, P.O. Box 3000, Boulder, CO 80307.]

Tsou, C.-H., and P. J. Smith, 1990: The role of synoptic/planetary-scale interactions during the development of a blocking anticyclone. *Tellus*, **42,** 174–193.

Vautard, R., and B. Legras, 1988: On the source of midlatitude low-frequency variability. Part II: Nonlinear equilibration of weather regimes. *J. Atmos. Sci.*, **45,** 2845–2867.

Waugh, D. W., 1993a: Contour surgery simulations of a forced polar vortex. *J. Atmos. Sci.*, **50,** 714–730.

——, 1993b: Subtropical stratospheric mixing linked to disturbances in the polar vortex. *Nature*, **365,** 535–537.

——, and R. A. Plumb, 1994: Contour advection with surgery: A technique for investigating finescale structure in tracer transport. *J. Atmos. Sci.*, **51,** 530–540.

——, ——, R. J. Atkinson, M. R. Schoeberl, L. R. Lait, P. A. Newman, M. Loewenstein, C. R. Webster, and R. D. May, 1994: Transport of material out of the stratospheric Arctic vortex through Rossby wave breaking. *J. Geophys. Res.*, **99,** 1071–1081.

Wolff, P. M., 1958: The error in numerical forecasts due to retrogression of ultra-long waves. *Mon. Wea. Rev.*, **86,** 245–250.